ASA, CSSA, and SSSA Virtual Issue Call for Papers:

Advancing Resilient Agricultural Systems: Adapting to and Mitigating Climate Change

Content will focus on resilience to climate change in agricultural systems, exploring the latest research investigating strategies to adapt to and mitigate climate change. Innovation and imagination backed by good science, as well as diverse voices and perspectives are encouraged. Where are we now and how can we address those challenges? Abstracts must reflect original research, reviews and analyses, datasets, or issues and perspectives related to objectives in the topics below. Authors are expected to review papers in their subject area that are submitted to this virtual issue.

Topic Areas

- Emissions and Sequestration
  - » Strategies for reducing greenhouse gas emissions, sequestering carbon
- Water Management
  - » Evaporation, transpiration, and surface energy balance
- Cropping Systems Modeling
  - » Prediction of climate change impacts
  - » Physiological changes
- Soil Sustainability
  - » Threats to soil sustainability (salinization, contamination, degradation, etc.)
  - » Strategies for preventing erosion
- Strategies for Water and Nutrient Management
  - » Improved cropping systems
- Plant and Animal Stress
  - » Protecting germplasm and crop wild relatives
  - » Breeding for climate adaptations
  - » Increasing resilience
- Waste Management
  - » Reducing or repurposing waste
- Other
  - » Agroforestry
  - » Perennial crops
  - » Specialty crops
  - » Wetlands and forest soils

Climate Change Virtual Issue

Submit Now!

Deadlines

Abstract/Proposal Deadline: Ongoing
Submission deadline: 31 Dec. 2022

How to submit

Submit your proposal to manuscripts@sciencesocieties.org

Please contact Jerry Hatfield at jerryhatfield67@gmail.com with any questions.

American Society of Agronomy | Crop Science Society of America | Soil Science Society of America

Received: 11 February 2021 | Accepted: 24 September 2021 | Published online: 22 December 2021

DOI: 10.1002/csc2.20652

Crop Science

ORIGINAL RESEARCH ARTICLE

Crop Physiology & Metabolism

Ecophysiological modeling of yield and yield components in winter wheat using hierarchical Bayesian analysis

Pratishtha Poudel[1] | **Nora M. Bello**[2] | **David A. Marburger**[3] | **Brett F. Carver**[1] | **Ye Liang**[4] | **Phillip D. Alderman**[1]

[1] Dep. of Plant and Soil Sciences, Oklahoma State Univ., 371 Agricultural Hall, Stillwater, OK 74078, USA

[2] Dep. of Statistics, Kansas State Univ., Room 002 Dickens Hall, 1116 Mid-Campus Drive N, Manhattan, KS 66506, USA

[3] FMC Midwest Research Station, 13239 IL Route 38, Rochelle, IL 61068, USA

[4] Dep. of Statistics, Oklahoma State Univ., 301 MSCS Bldg, Stillwater, OK 74078, USA

Correspondence
Phillip D. Alderman, Dep. of Plant and Soil Sciences, Oklahoma State Univ., 371 Agricultural Hall, Stillwater, OK 74078, USA.
Email: phillip.alderman@okstate.edu

Assigned to Associate Editor John Foulkes.

Abstract

Yield components are widely recognized as drivers of wheat (*Triticum aestivum* L.) yield across environments and genotypes. In this study, we used a hierarchical Bayesian approach to model wheat grain yield in Oklahoma on an eco-physiological basis using yield component traits thousand kernel weight (TKW) and nonyield biomass (NYB). The Bayesian approach allowed us to quantify uncertainties around the parameter values rather than obtaining a single value estimate for a parameter. The main objectives of this study were to (a) explain wheat yield as a function of component traits TKW and NYB, and thereby examine the implications for source-sink balance; and (b) assess their association with weather conditions during key stages of wheat development. A secondary objective was to introduce Bayesian estimation for eco-physiological modeling. Fifteen wheat genotypes planted in three locations in Oklahoma (Altus, Chickasha, and Lahoma) were evaluated across three harvest years (2017 to 2019), whereby the combination of location and year defined an environment. Results indicate that the environment explained a greater proportion of the variability in yield than genotypes or than genotype × environment (G × E) interaction; however, evidence for G × E was substantial. Yield was expected to increase with increasing TKW and NYB, which would suggest a source limitation to achieve potential yield. Yet, the contribution of early reproductive stage weather variables to the relationship between yield and NYB pointed in the direction of sink strength being compromised. In summary, our approach provides evidence for source-sink co-limitation in grain yield of this sample of hard red winter wheat genotypes.

1 | INTRODUCTION

Wheat (*Triticum aestivum L.*) is a staple food crop in many countries that supplies the most calories and protein to the population worldwide (Peña-Bautista et al., 2017). However, wheat genotypes, wheat-growing environments, and wheat yields differ worldwide across regions, years, and growing

Abbreviations: elpd, expected log predictive density; G × E, genotype × environment; HDI, highest posterior density interval; HI, harvest index; MCMC, Markov chain Monte Carlo; NYB, nonyield biomass; OSU, Oklahoma State University; PPI, posterior probability interval; RMSE, root mean squared error; SKCS, single kernel characterization system; TKW, thousand kernel weight.

seasons. Climate variation was found to explain 32–39% of interannual yield variability in maize, rice, wheat, and soybean globally (Ray et al., 2015). Yield variability exists not only between different regions in the world but also within the specific regions across locales and growing seasons. Understanding the mechanisms behind yield variability within a wheat-growing region would allow breeding programs to develop wheat genotypes tailored to reduce the gap between the maximum attainable yield and observed yield.

This study was conducted in the United States in the state of Oklahoma. The wide range of environments across the state makes it an ideal region to study yield variability as a result of variable weather conditions. A wide range of environmental conditions are present in Oklahoma, driven mostly by a temperature gradient from south to north and a precipitation gradient from east to west, along with yearly fluctuations in temperature and precipitation patterns (Tian & Quiring, 2019). As a result, wheat yields are variable across the state (Calhoun et al., 2019; USDA, 2019). For instance, in 2019, wheat yield ranged from 1.8 ton/ha in Southwest Oklahoma to 4.2 ton/ha in East Central Oklahoma (USDA, 2019).

Environmental effects, different genotypes, and genotype × environment (G × E) interactions play an important role in explaining yield variability (Mohammadi et al., 2010; Roozeboom et al., 2008). Specifically, G × E effects on wheat yield are ultimately driven by different physiological mechanisms. For instance, the crop environment at the early reproductive stages of plant growth impacts wheat yield primarily through changes in grain number (Fischer, 1985; Ugarte et al., 2007) whereas the environmental conditions during anthesis and the grain filling stage can affect wheat yield mainly via changes in grain size (Serrago & Miralles, 2014; Wardlaw & Moncur, 1995). These traits are simultaneously driven by the combined effects of genetics and environmental impact, thus leading to G × E interaction.

Multienvironment trials are a well-established component of crop breeding programs to study G × E interactions. These trials are important to characterize the performance of wheat genotypes over a wide range of environments. In this study, we utilize data from the Oklahoma Small Grains Variety Performance Tests, a multienvironment trial, conducted yearly by Oklahoma State University (OSU). Most multienvironment trials focus mainly on yield (Kaya et al., 2006; Mohammadi et al., 2010; Roozeboom et al., 2008; Sukumaran et al., 2017) as this is one of the more important outcomes of a cultivar, for which producers base their choice. Yet, yield data alone provide limited insight into the mechanisms for differential responses of genetic cultivars to changing environments. Grain yield is a function of multiple component traits including kernel weight and size, kernels per spike, spikes per tiller, and the number of tillers amongst others, each at different levels of trait plasticity (Slafer et al., 2014). Stable components of yield such as grain size are placed at the lowest level of trait plasticity denoting that they are mostly governed by genetic factors. In turn, components such as the number of tillers show high plasticity as they are highly influenced by the environment (Sadras & Slafer, 2012). We postulate that further partitioning of yield into its component traits could help explain the observed variability in yield and thus increase the quality of predictions.

Core Ideas

- Yield components serve as proxy for source and sink.
- Association of yield components with yield is mediated by weather conditions.
- Wheat yield is co-limited by source and sink.
- Bayesian hierarchical modeling naturally reflects hierarchy of biological systems.

Wheat yield can be effectively partitioned into two main yield component traits, namely grain number and average grain weight; these are modulated by a source-sink balance (Fischer, 2008; Ugarte et al., 2007). In most conditions, wheat is a sink-limited crop (Borrás et al., 2004). Sink limitations are due to stress during early reproductive stages, which leads to the setting of fewer grains than what can be filled later during grain filling. In contrast, postanthesis abiotic and biotic stresses can reduce grain size or weight; this is an example of a source-limited condition. The balance between source and sink is crucial to realizing yield potential.

Although analyses pertaining to understanding these systems through eco-physiological dynamics have been traditionally performed within a frequentist framework, some studies have utilized a Bayesian approach (Cotes et al., 2006; Cuevas et al., 2017; Montesinos-López et al., 2019). Bayesian hierarchical modeling provides a useful framework for exploring these interactions in several respects. First, the hierarchical structure of the model corresponds to the nature of the biological system under study. Second, a Bayesian framework provides a natural mechanism for incorporating what is already known about a given system in the form of prior distributions. For well-defined relationships, informative priors can be used; whereas for novel research questions, more diffuse priors can be constructed. Third, Bayesian analysis is increasingly being used due to its emphasis on quantifying posterior distributions for parameters of interest rather than point estimates alone (Alderman & Stanfill, 2017). These posterior distributions can be used to derive point estimates, if needed, along with a range of uncertainty around those estimates. Doing so provides a well-rounded perspective on the nature and strength of the relationships being explored.

Ultimately, our goal is to explain wheat yield variability on an eco-physiological basis. The main objectives of this study

TABLE 1 Wheat genotypes included in this study by season

Genotypes	2016–2017	2017–2018	2018–2019
Bentley		X	X
Billings	X		
Doublestop CL+	X	X	X
Duster	X	X	X
Endurance	X		
Gallagher	X	X	X
Iba	X	X	X
LCS Chrome		X	X
Lonerider		X	X
Ruby Lee	X	X	X
Smith's Gold		X	X
SY Achieve CL2		X	X
SY Flint	X	X	X
SY Llano	X		
WB4458	X	X	

were to (a) explain wheat yield as a function of component traits thousand kernel weight (TKW) and nonyield biomass (NYB), thus examine the implications for source-sink balance and (b) assess their association with weather conditions during key stages of wheat development. We leverage a hierarchical Bayesian modeling framework to naturally reflect the hierarchical features of the biological question. Thus, as a secondary objective, we introduce Bayesian estimation for ecophysiological modeling.

2 | MATERIALS AND METHODS

The samples for this study were collected from the Oklahoma Small Grains Variety Performance Tests conducted by OSU on a yearly basis. The OSU wheat cultivar testing program features replicated trials at more than 20 different test sites and nonreplicated trials at more than 40 demonstration sites, representing major wheat-growing areas in the state.

2.1 | Wheat genotypes included in this study

For this study, we selected wheat genotypes based on acreage planted in Oklahoma (Table 1). Some of the genotypes included in this study changed across years as newer cultivars replaced older ones. The genotypes selected for this study showed a range of plant heights, maturity, yield potential, disease resistance, test weight, kernel size, drought tolerance, Hessian fly resistance, and dual-purpose suitability, but all were intended to represent the diversity of wheat grown in Oklahoma (Marburger et al., 2018; OSU Small Grains Extension, 2020). For example, the wheat genotypes 'Doublestop CL+', 'Endurance', and 'Iba' (Marburger et al., 2021) were chosen for their late maturity, whereas 'Gallagher' (Marburger et al., 2021), 'Lonerider', 'SY Achieve CL2', and 'SY Llano' were chosen for their early maturity; meanwhile, 'Billings' (Edwards et al., 2012), 'SY Flint', and 'WB4458' were chosen for their medium-early maturity. Likewise, Billings has a high grain-only yield potential but is not suitable for dual-purpose systems (Hunger et al., 2014) whereas Smith's Gold has excellent yield potential and is suitable for both grain-only and dual-purpose production systems. Bentley has yield stability under drought conditions but lower test weight, and Doublestop CL+ has yield stability across a wide range of environments along with high test weight (OSU Small Grains Extension, 2020). The genotypes also differ in disease resistance; Billings, 'Duster' (Edwards et al., 2012), Gallagher, Iba, and 'LCS Chrome' exhibit good stripe and leaf rust (caused by *Puccinia striiformis* and *Puccinia triticina*) resistance, whereas Bentley, Doublestop CL+, Endurance, Smith's Gold, and SY Flint are moderately resistant. Meanwhile, 'Ruby Lee' is moderately susceptible to stripe rust only. Furthermore, Duster has above-average tillering capacity with intermediate straw strength, whereas LCS Chrome has both high tillering ability and good straw strength (Marburger, Hunger, et al., 2018).

2.2 | Sites and management description

For this study, a total of three sites were selected for sample collection from the set of locations within the OSU the Oklahoma Small Grains Variety Performance Tests, namely Altus, Chickasha, and Lahoma. The selected sites represent diversity in latitude, longitude, elevation, climatic conditions, and soil types across the state (Table 2). The seasonal rainfall and temperature estimates for the months of October through June were calculated from the preceding 15 yr of data (2003-=2004 to 2018–2019) obtained from nearby stations of the Oklahoma Mesonet (Brock et al., 1995; McPherson et al., 2007). All trials were conducted as a randomized complete block design with four replicates using a conventional tillage system. Trials at each site followed standard management practices for the area, with a 67 kg ha^{-1} seeding rate and 56 kg ha^{-1} of 18-46-0 (N–P_2O_5–K_2O) applied in-furrow at the time of planting, using a Hege 500 small-plot cone seeder (Wintersteiger). Each plot consisted of eight rows spaced 15 cm apart.

2.3 | Experimental design and data collection

Data were collected at the three sites over the course of three growing seasons (2016–2017, 2017–2018, and 2018–2019),

TABLE 2 Description of experimental sites included in the study

Site	Latitude	Longitude	Elevation	Rainfall	Temperature	Soil type
			m	mm	˚C	
Altus	34.63˚ N	99.33˚ W	426	388	12 ± 7.94	Hollister silty clay loam
Chickasha	35.05˚ N	97.94˚ W	339	534	11.1 ± 7.9	Dale silt loam
Lahoma	36.39˚ N	98.09˚ W	380	437	9.87 ± 8.16	Pond creek silt loam

Note. Average seasonal cumulative rainfall (Rainfall) and average seasonal temperature (Temperature) from October through June calculated from the preceding 15 yr of data (2003–2004 to 2018—2019) obtained from nearby Oklahoma Mesonet stations

excluding Altus in 2016–2017. Thus, we used the combination of site and year to define eight environments. A total of 10 genotypes were sampled in the first year, 12 in the second year, and 11 in the third year from each site. Thus, not all genotypes were observed in all environments.

From each plot in each of the four field replicates, a meter row of the selected genotypes (0.5 m on two second from outer rows) was hand-harvested at physiological maturity with a sickle at ground level to produce one sample per plot. Samples were dried for 72 h at 60 ˚C. An ALMACO Plant and Head Thresher (Allan Machine Company) was used to thresh the samples, and dry biomass and grain weights were recorded for each plot. Yield (g m^{-2}) was calculated from sample grain weight. Nonyield biomass (g) was calculated as the sample grain weight (g) subtracted from the total sample biomass (g).

Average kernel weight (mg) was obtained for each sample using the Single Kernel Characterization System 4100 (SKCS, Perten Instruments North America Inc.) following standard operating procedures as outlined in the instruction manual (Perten Instruments, 1995). From sample of approximately 20 g per field plot, the SKCS 4100 provided a mean, standard deviation, and distribution for single kernel weight (mg) of 300 machine-singulated sound kernels (Martin et al., 1993; Osborne & Anderssen, 2003). Thousand kernel weight (g) was calculated from the mean obtained for SKCS kernel weight.

Data on weather variables, daily values of minimum and maximum temperatures (˚C), precipitation (mm), and solar radiation (M Jm^{-2}), were obtained from the Oklahoma Mesonet for each location and year (Brock et al., 1995; McPherson et al., 2007). The air temperature was calculated as the average of minimum and maximum temperatures. Cumulative precipitation, average solar radiation, and average air temperature were calculated to summarize the weather variables over two growth periods per season to represent the early reproductive stage (from 6 wk prior to the heading date, corresponding to Zadok's growth stage 59, until 2 wk after the heading date) and grain filling stage (from 2 wk after the heading date until 2 wk prior to the harvest date, Zadok's growth stage 93) for each trial. Heading dates and harvest dates were obtained from the variety performance trial reports (Calhoun et al., 2019; Marburger et al., 2017; Marburger, Calhoun, Carver, et al., 2018).

2.4 | Model specification and data analysis

Although the individual field trials followed a randomized complete block design design, the combination of multiple trials for data analysis reflected a split-plot like structure where the field trials served as main plots. Each field trial corresponds to a unique site–year combination or environment as described above. A basic statistical model was specified to reflect the structure of the whole dataset. Specifically, random effects included in the linear predictor were environment, block nested within an environment (the blocking structure for genotypes), genotype, and G × E. The residual represented the remaining noise at the individual plot level. Three alternative models were specified according to the objective of explaining yield as a function of its component traits, namely:

Alternative 1: Model including G × E effects (Model GE):

$$Y_{ijk} = \beta_0 + Env_k + Geno_j + [Geno * Env]_{jk} + Block[Env]_{i[k]} + e_{ijk}$$

where Y_{ijk} = observed yield (g m^{-2}) from the plot corresponding to the *i*th block ($i = 1, \ldots, 4$) in the *k*th environment (k = 1, …, 8) planted with the *j*th genotype (j = 1, …, 15) and β_0 = overall intercept, interpretable as expected yield for a "typical" genotype in a "typical" environment, whereby typical is defined as the population expectation for genotypic effects, environmental effects and their combination, that is,

$$E\left(Geno_j\right) = E\left(Env_k\right) = E(Geno * Env)_{jk} = 0$$

where $Geno_j$ = differential effect of the *j*th genotype, assumed $Geno_j \sim NIID(0, \sigma^2_{geno})$; Env_k = differential effect of the *k*th) environment, assumed $Env_k \sim NIID(0, \sigma^2_{env})$; and $[Geno*Env]_{jk}$ = differential effect of the *j*th genotype planted in the *k*th environment, assumed $[Geno * Env]_{jk} \sim NIID(0, \sigma^2_{ge})$.

$Block[Env]_{i[k]}$ = differential effect of the *i*th block nested within the *k*th environment and assumed $Block[Env]_{i[k]} \sim NIID(0, \sigma^2_b)$ and e_{ijk} = residual unique to the observation collected on ijk^{th} plot and assumed $e_{ijk} \sim NIID(0, \sigma^2_r)$.

Alternative 2: Model including effects of G × E and yield components (Model GE-YC):

$$Y_{ijk} = \beta_0 + Env_k + Geno_j + \beta_1 * nyb_{ijk} + \beta_2 * tkw_{ijk} + [Geno * Env]_{jk} + Block[Env]_{i[k]} + e_{ijk}$$

where $Y_{ijk}, \beta_0, Env_k, Geno_j, [Geno * Env]_{jk}, Block[Env]_{i[k]}$, and e_{ijk} are as previously defined for model GE. nyb_{ijk} = observed NYB corresponding to the plot in the ith block of the kth environment planted with the jth genotype, and expressed as the deviation from its mean; tkw_{ijk} = observed TKW corresponding to the plot in the ith block of the kth environment planted with the jth genotype, and expressed as the deviation from its mean; β_1 = slope coefficient, indicating the rate of change of yield per unit increase in NYB, for a typical genotype and environment as previously defined; and β_2 = slope coefficient, indicating the rate of change of yield per unit increase in TKW for a typical genotype and environment as previously defined.

Alternative 3: Model including G × E and a hierarchical specification of yield components (Model GE-YC-hierarchy):

$$Y_{ijk} = \beta_0 + Env_k + Geno_j + \beta_{nyb,k} * nyb_{ijk} + \beta_{tkw,k} * tkw_{ijk} + [Geno * Env]_{jk} + Block[Env]_{i[k]} + e_{ijk}$$

with a hierarchical specification of yield components such that:

$$\beta_{nyb,k} = \beta_{10} + \beta_{11} * temp1_k + \beta_{12} * srad1_k + \beta_{13} * rain1_k$$
$$\beta_{tkw,k} = \beta_{20} + \beta_{21} * temp2_k + \beta_{22} * srad2_k + \beta_{23} * rain2_k$$

where $Y_{ijk}, \beta_0, Env_k, Geno_j, [Geno * Env]_{jk}, Block[Env]_{i[k]}$, and e_{ijk} are as previously defined for model GE; and nyb_{ijk} and tkw_{ijk} are as previously defined for model GE-YC. $temp1_k$, $srad1_k$, $rain1_k$ = temperature, solar radiation, and precipitation, respectively, for the k^{th} environment during the early reproductive growth stage, expressed as the deviations from their respective means. $temp2k, srad2_k, rain2_k$ = temperature, solar radiation, and precipitation, respectively, for the kth environment, during the grain filling stage, expressed as the deviations from their respective means. β_{10} = intercept for the hierarchical specification of NYB, indicating the expected rate of change of yield per unit increase in NYB for a typical genotype at average temperature, precipitation, and solar radiation for the early reproductive growth stage. β_{11}, β_{12}, β_{13} = expected change in the slope of NYB on yield per unit increase of temperature, solar radiation, and precipitation, respectively, during the early reproductive growth stage. β_{20} = Intercept for the hierarchical specification of TKW, indicating the expected rate of change of yield per unit increase in TKW for a typical genotype at average temperature, precipitation, and solar radiation during the grain filling stage. B_{21}, β_{22}, β_{23} = Expected change in the slope of TKW on yield per unit increase of temperature, solar radiation, and precipitation, respectively, during the grain filling stage.

For data analyses, the statistical models were fitted using a hierarchical Bayesian framework.

2.5 | Prior specification

Specification of priors for all hyperparameters was performed using the prior predictive checks approach proposed by Schad et al. (2019). Briefly, hyperparameters were included in the prior predictive model in a stepwise fashion of increasing model complexity, following model hierarchy from Alternative Models 1 to 3. At each step, prior predictive checks were performed to ensure that predictions from the priors were within a biologically plausible, though vague, boundary. The boundary was set based on the average wheat yields throughout the world and was allowed to vary up to around 1,800 g m^{-2}, which could be considered weakly informative given that it is in excess of maximum observed wheat yields globally. A prior predictive check was conducted by sampling from the defined priors and simulating model predictions for the variable of interest based on those samples. If the predictions were biophysically plausible, the priors passed the check, but if the priors produced nonsense predictions, priors were revised to produce predictions aligned with our beliefs and prior knowledge about the system under study. Prior specifications for vague predictions were intended to put the weight of posterior inference on the actual data. Prior specifications for parameters in modeling Alternatives 1–3 are presented next in the form of $Normal(\mu, \sigma^2)$, such that:

$$\beta_0 \sim Normal(300, 80^2)$$

$$\beta_1 \sim Normal(0, 1^2)$$

$$\beta_2 \sim Normal(0, 15^2)$$

$$\beta_{10} \sim Normal(0, 0.5^2)$$

$$\beta_{20} \sim Normal(0, 15^2)$$

$$\beta_{11} \sim Normal(0, 0.1^2)$$

$$\beta_{12} \sim Normal(0, 0.05^2)$$

$$\beta_{13} \sim Normal(0, 0.1^2)$$

$$\beta_{21} \sim Normal(0, 1^2)$$

$$\beta_{22} \sim Normal(0, 0.5^2)$$

$$\beta_{23} \sim Normal(0, 1^2)$$

$$\sqrt{\sigma^2_{env}} \sim Truncated\ normal(0, 150^2) \text{ such that } \sqrt{\sigma^2_{env}} > 0$$

$$\sqrt{\sigma^2_{geno}} \sim Truncated\ normal(0, 80^2) \text{ such that } \sqrt{\sigma^2_{geno}} > 0$$

$$\sqrt{\sigma^2_{ge}} \sim Truncated\ normal(0, 100^2) \text{ such that } \sqrt{\sigma^2_{ge}} > 0$$

$$\sqrt{\sigma^2_{b}} \sim Truncated\ normal(0, 50^2) \text{ such that } \sqrt{\sigma^2_{b}} > 0$$

$$\sqrt{\sigma^2_{r}} \sim Truncated\ normal(0, 250^2) \text{ such that } \sqrt{\sigma^2_{r}} > 0$$

2.6 | Software implementation

Statistical models were fitted using a hierarchical Bayesian framework based on Hamiltonian Monte Carlo as implemented by the software Stan (Stan Development Team, 2018) through the R statistical software environment (R Core Team, 2020; Stan Development Team, 2019). For each model, four Markov chain Monte Carlo (MCMC) chains with 10,000 iterations and 50% burn-in were run, resulting in a total of 20,000 saved iterations for posterior inference. Traceplots and R-hat values were used to monitor chain convergence (Gelman et al., 2013). Auto-correlations and effective sample size for key lower-level parameters were computed. Specifically, the MCMC chains were tuned to ensure that effective sample size for the hyperparameters σ_{geno}, σ_{env}, σ_{ge}, and σ_b was greater than 3,000 in all models.

Figures were generated using the ggplot2 package in R (Wickham, 2016). The highest posterior density intervals (HDIs) were computed using the HDInterval package (Meredith & Kruschke, 2018). Figures and tables were generated or rendered using the R packages knitr (Xie, 2020) and kableExtra (Zhu, 2019). The R package tidyverse was used for data cleaning and organization (Wickham et al., 2019; Wickham, 2017).

The computing for this project was performed on the TIGER research cloud at the Oklahoma State University High Performance Computing Center using a KVM virtual machine backed by a hypervisor node with dual Intel "Skylake" 6,130 CPUs and 768 GB RAM.

2.7 | Bayesian approach to data analysis

In Bayesian data analyses, estimation of parameters of interest and subsequent inference, as well as predictions, come in the form of posterior densities that are obtained numerically from the MCMC. In contrast, the reader may recall that deterministic methods produce parameter-specific point estimates only. The availability of posterior densities is highly desirable as it provides considerably more information about the parameters of interest (or functions thereof), thus enabling not only point estimation but also assessments of uncertainty. Specifically, from a posterior density, one may select amongst a number of possible location descriptors for the most appropriate point estimate, say mean, median, or mode, depending on the symmetry (or lack thereof) of the posterior density for the parameter of interest. Even more compelling is the fact that posterior densities also enable an assessment of uncertainty around the selected point estimator (Gelman et al., 2013). In a statistical sense, uncertainty is an indicator of precision of the estimate based on the amount of information available in the data, and thus, an indicator of how likely we are to reproduce those estimates under similar conditions. For example, posterior intervals such as HDI, or alternatively, posterior probability interval (PPI), indicate the range of values within which one can expect to find the parameter of interest with 95% probability (Gelman et al., 2013). These intervals may be considered analogous to the concept of confidence intervals in frequentist statistics, though their Bayesian interpretation is straightforward, thus more intuitive and directly aligned with research objectives. That is, we are 95% confident that the parameter takes values contained within the boundaries of the interval. Specifically, a 95% PPI is the interval in the distribution that contains the middle 95% of the posterior samples and thus has equal tails (Gelman et al., 2013). In turn, the HDI of a posterior distribution is the shortest possible interval which captures 95% of the posterior samples with the highest probability densities (Grieve, 1991). It is worth noting that this statistical definition of uncertainty on individual parameters or individual predictions is different from variability across model-derived point predictions.

In this article, we report posterior summaries for each parameter of interest (and functions thereof) using posterior medians and 95% HDI.

2.8 | Model comparison

Model 3: GE-YC-hierarchy was our model of preference, because its hierarchical nature offers insights into relevant physiological mechanisms. The model comparison was performed to determine if the added complexity in Model 3: GE-YC-hierarchy compromised the predictive ability of the

model. Alternative models were compared using statistical metrics for goodness-of fit and predictive ability. Specifically, Bayesian R-squared and root mean square error (RMSE) were calculated to assess goodness-of-fit, and expected log predictive density (elpd) was calculated in a q-fold cross-validation with Q = 10 for each alternative model. Approximately 315 data points were used as training vs. 35 holdout data points for each fold of cross-validation.

First, a Bayesian R-squared statistic was calculated for each MCMC iteration (s) as described in Gelman et al. (2019), such that:

$$Bayesian\ R_s^2 = \frac{var(\hat{y})^s}{var(\hat{y})^s + \sigma_r^{2\,s}}$$

where, $var(\hat{y})$ = variance between predicted values at iteration s, whereby s = 1, 2, …, S is the length of post-burnin MCMC, $\sigma_r^{2\,s}$ = Posterior sample of residual variance (σ_r^2) for each MCMC iteration s.

Then, RMSE was also calculated for each MCMC iteration (s) as:

$$RMSE_s = \sqrt{\frac{1}{N}\sum_{n=1}^{N}(y_n - \hat{y}_n^s)^2}$$

where, N = Total number of data points, y_n = nth observation, and $\hat{y}_n$ = Predicted value for the nth observation sampled in MCMC iteration s.

Finally, elpd was calculated following Equations 20 and 21 in Vehtari et al. (2017) such that:

$$elpd = \sum_{q=1}^{Q}\sum_{m=1}^{M_q} log\left[\frac{1}{S}\sum_{s=1}^{S} p(y_m|\theta^{-q,s})\right]$$

where Q = the number of folds, M_q = number of observations within the qth fold, S = number of saved post burnin MCMC iterations, y_m = data point m within the qth fold, and $\theta^{-q,s}$ = parameters corresponding to the qth holdout subset and iteration s, and $p(y_m|\theta{-}^{q,s})$ = probability of y_m given $\theta^{-q,s}$.

Models with smaller values of RMSE, and with larger values of Bayesian R-squared, and elpd were considered preferable.

3 | RESULTS

3.1 | Model comparison

Table 3 shows selected criteria used for model comparison, specifically, Bayesian R-squared and RMSE to assess goodness-of-fit, and elpd to assess the predictive ability of each alternative model considered. Smaller Bayesian R-squared and larger RMSE both indicate impaired fit of Model 1: GE relative to Model 2: GE-YC and Model 3: GE-YC-hierarchy, thus clearly suggesting a preference for the latter two. Meanwhile, Model 3: GE-YC-hierarchy showed the the largest value of Bayesian R-squared and the smallest RMSE. Yet, numerical differences in both fit criteria were minor relative to Model 2: GE-YC, thus indicating little evidence for preference of either model over the other in terms of relative fit to data.

In terms of predictive ability, Model 3: GE-YC-hierarchy performed best, as supported by the largest elpd value, followed closely by Model 2: GE-YC, and lastly by Model1: GE. Model 3: GE-YC-hierarchy and Model 2: GE-YC showed a minor difference in predictive ability, as indicated by an elpd difference close to zero and of smaller magnitude than the standard error of such difference, indicating inadequate evidence in favor of any one model in terms of predictive ability. For further inference, we made the decision to proceed with Model 3: GE-YC-hierarchy based on a combination of (a) best or comparable fit relative to other model alternatives considered in this study, and (b) its hierarchical nature, which enables insight into specific physiological mechanisms contributing to yield differences without compromising predictive ability.

Figure 1 illustrates the posterior density of the Bayesian R-squared for Model 3 G × E and yield component (GE-YC) hierarchy selected for further inference. Notably, the 95% HDI for Bayesian R-squared for this model had a lower bound of 0.88 and an upper bound of 0.91, indicating a 95% probability that Model 3: GE-YC-hierarchy captures somewhere between 88–91% of the variability observed in the data.

3.2 | Genotypic, Environmental, and G × E effects on wheat yield

Table 4 shows posterior inference of variance components for genotypic (σ^2_{geno}), environmental (σ^2_{env}) and G × E effects (σ^2_{ge}), as well as residual-level (σ^2_r), for the alternative models considered in this study. As expected, the addition of NYB and TKW as explanatory variable to Model 2: GE-YC and Model 3: GE-YC-hierarchy caused a substantial decrease of approximately one order of magnitude in the residual variance (σ^2_r) and the environmental variance (σ^2_{env}) compared with Model 1: GE. Based on the posterior medians for Model 3: GE-YC-hierarchy, σ^2_{env} showed the greatest magnitude with six times σ^2_{geno} or σ^2_{ge} (Table 4). When comparing the point estimates (medians) for genotype-specific and G × E effects, their magnitudes appear similar; however, upon further analysis it was found that there is a 61.6% probability that the genotype-specific effects were higher than the G × E effects.

TABLE 3 Model comparison based on Bayesian R-squared, and root mean square error (RMSE; expressed as highest posterior density interval [HDI]), and difference in expected log predictive density (elpd_diff ± SE) for Model 1 genotype × environment (GE), Model 2 GE and yield component (GE-YC), and Model 3 GE and YC with hierarchy (GE-YC-hierarchy)

	Bayesian R-squared		RMSE		
Models	**Median**	**HDI**	**Median**	**HDI**	**elpd_diff ± SE.**
1. GE	0.759	(0.718, 0.799)	103.48	(98.29, 109.05)	−142.6 ± 28.0
2. GE-YC	0.896	(0.877, 0.914)	67.86	(64.42, 71.88)	−3.6 ± 28.3
3. GE-YC-hierarchy	0.899	(0.880, 0.917)	66.77	(63.06, 70.71)	0

Note. Values for elpd_diff are expressed relative to GE-YC-hierarchy(e.g., elpd_diff for GE is elpd for GE-YC-hierarchy subtracted from elpd for GE).

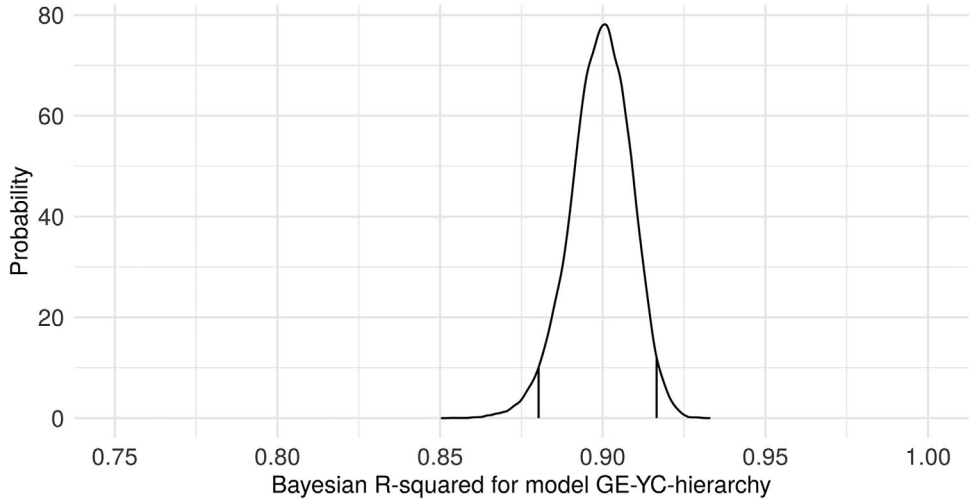

FIGURE 1 Posterior distribution of Bayesian R-squared and 95% HDI as indicated by the vertical lines in the density plot

TABLE 4 Posterior summary (posterior median and 95% highest posterior density interval [HDI]) on variance components: Genotype (σ^2_{geno}), environment (σ^2_{env}), genotype × environment interaction (σ^2_{ge}), and residuals (σ^2_r) for alternative models

	σ^2_{geno}		σ^2_{env}		σ^2_{ge}		σ^2_r	
Models	**Median**	**HDI**	**Median**	**HDI**	**Median**	**HDI**	**Median**	**HDI**
1. GE	1,102.54	(0.01, 3,158.75)	39,574.91	(11,592.48, 93,647.42)	1,087.51	(0.0006, 2,746.35)	10,760.34	(8,937.15, 12,875)
2. GE-YC	1,181.33	(170.21, 3,098.04)	4,686.17	(428.28, 17,098.25)	1,218.47	(337.99, 2,031.73)	4,637.45	(3,849.4, 5,566.9)
3. GE-YC-hierarchy	1,280	(184.33, 3,192.07)	7,918.37	(1,123.51, 27,753.57)	1,068.13	(282.38, 1,974.75)	4,490	(3,686.04, 5,370.17)

Note. GE, genotype × environment; GE-YC, genotype × environment and yield components.

Figure 2 illustrates the posterior median of environment-specific yield predictions for each of the wheat genotypes present in all environments in this study. All predictions were obtained using results from Model 3: GE-YC-hierarchy. Specifically, the left panel depicts predictions based on effects of genotype, environment, and G × E at average values of NYB and TKW, whereas the right panel depicts predictions based on effects of G, E, and G × E at values of NYB and TKW specific to that environment. Both panels depict presence of G × E interaction on wheat yield, as indicated by the change in rank of the genotypes across environments. The difference in G × E patterns depicted by the two panels may be explained by the fact that the contributions of NYB and TKW represent a portion of the G × E interaction that is attributable to the eco-physiological processes for which they are proxies. Whereas the term G × E stated explicitly in Model 3: GE-YC-hierarchy may be interpreted as the remaining unattributable portion of the environment-specific genotype effect on wheat yield.

3.3 | Association between yield component traits and wheat yield

Table 5 shows posterior summaries for location parameters (β) of Model 3: GE-YC-hierarchy across hierarchical levels.

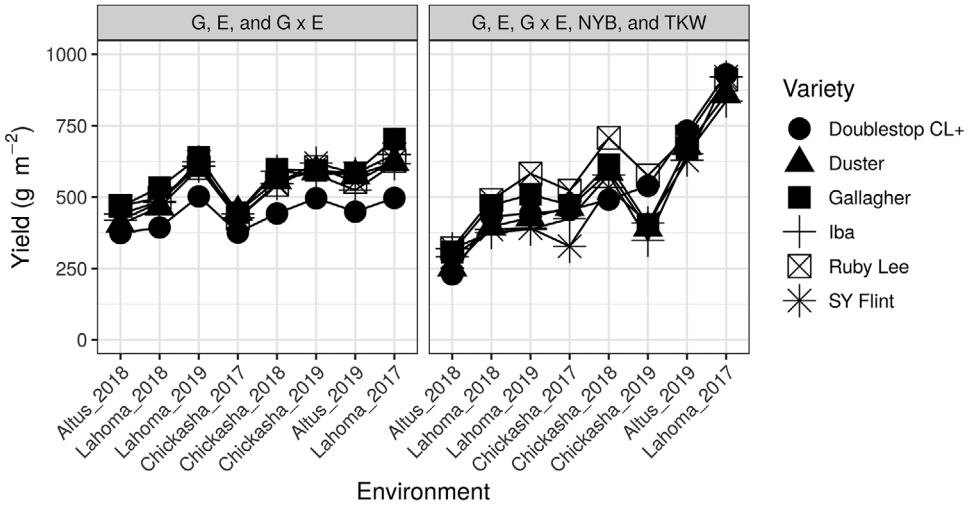

FIGURE 2 Predicted wheat yield for selected genotypes across environments based on Model 3: genotype × environment and yield components with hierarchy (GE-YC- hierarchy), considering (left panel) genotype (G), environment (E), and G × E effects at average NYB and TKW, and (right panel) G, E, G × E effects, as well as nonyield biomass (NYB), and thousand kernel weight (TKW) at the corresponding environments (i.e., shown as site-harvest year combinations)

TABLE 5 Posterior median and highest density posterior interval (HDI) for the intercept and the regression coefficients in the model with genotype × environment and yield components with hierarchy (GE-YC-hierarchy)

Parameter	Description	Median	HDI
β_0	Yield at typical conditions	490	(404, 557)
β_{10}	Expected change in yield per unit increase in NYB under average weather conditions during early reproductive stage	0.43	(0.38, 0.47)
β_{20}	Expected change in yield per unit increase in TKW under average weather conditions during grain filling stage	13	(9, 16)
β_{11}	Change in β_{10} per unit increase in early reproductive stage temperature	0.01	(−0.029, 0.054)
β_{12}	Change in β_{10} per unit increase in early reproductive stage solar radiation	0.05	(0.006, 0.098)
β_{13}	Change in β_{10} per unit increase in early reproductive stage precipitation	0.01	(−0.001, 0.020)
β_{21}	Change in β_{20} per unit increase in grain filling stage temperature	−0.14	(−1.425, 1.123)
β_{22}	Change in β_{20} per unit increase in grain filling stage solar radiation	−0.002	(−0.961, 0.960)
β_{23}	Change in β_{20} per unit increase in grain filling stage precipitation	0.32	(−0.140, 0.789)

Note. NYB, nonyield biomass; TKW, thousand kernel weight.

As a benchmark reference, we articulate that the posterior inference for β_0 indicates that yield for a "typical" genotype member of the population in a "typical" environment, that is, $E(Geno_j) = E(Env_k) = E([Geno * Env]_{jk}) = 0$, at average values of NYB and TKW can be expected to be approximately 490 g m^{-2}, ranging from 404 to 557 g m^{-2}, with 95% probability.

Furthermore, posterior inference on β_{10} and $\beta 2_0$ indicates that one may expect the behavior of wheat yield to change as a function of the source-sink balance represented here by NYB and TKW (Table 5). Specifically, posterior inference on β_{10} indicates an expected increase in yield per unit increase in NYB of approximately 0.43 g m^{-2} and ranging from 0.38 to 0.47 g m^{-2} with 95% probability with typical weather conditions during the early reproductive growth stage. The values for NYB in this dataset ranged from 325 to 2,326 g m^{-2}. Taking this range into account, one can expect the yield to change by 140 to 1,000 g m^{-2} as a result of change in NYB. Likewise, posterior inference on β_{20} supports an expected increase in yield per unit increase in TKW of approximately 13 g m^{-2}, ranging from 9 to 16 g m^{-2}, with 95% probability at typical weather conditions during the grain-filling stage. Taking into account the range for TKW in this dataset (14 to 39 g), the yield can be expected to change by 182 to 507 g m^{-2} as a result of change in TKW.

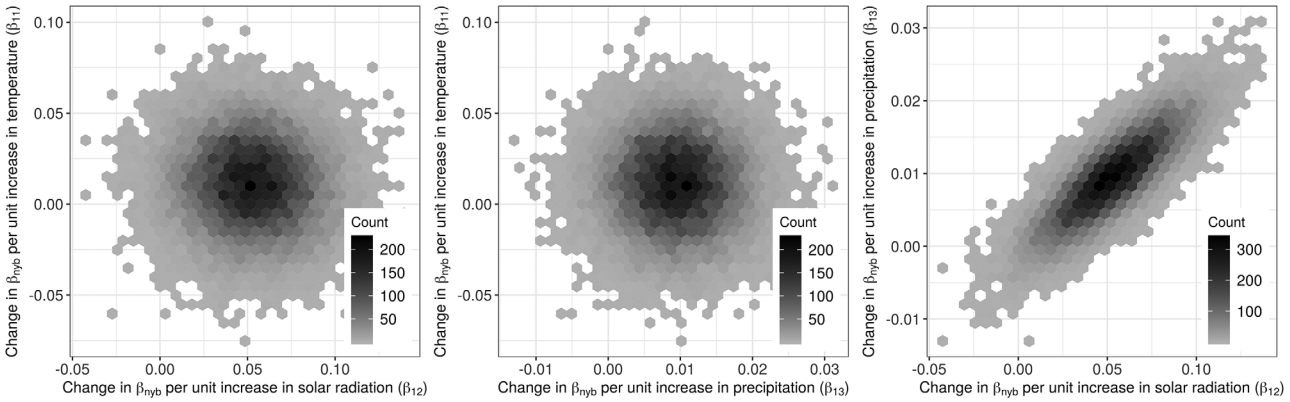

FIGURE 3 Pairwise joint posterior densities for parameters β_{11}, β_{12}, β_{13} characterizing the contribution of weather variables to the relationship between yield and nonyield biomass during the early reproductive stage

3.4 | Contribution of weather variables to the relationships between yield and yield component traits

Table 5 presents posterior summaries on parameters β_{11}, β_{12}, β_{13}, which characterize the contribution of temperature, solar radiation, and precipitation, respectively, to wheat yield through NYB during the early reproductive stage, allowing us to look into source-sink balance in the population. Specifically, at the early reproductive stage, solar radiation showed a positive effect on β_{nyb}, that is the expected rate of change of wheat yield as a function of NYB, as indicated by the positive sign of both boundaries of 95% HDI of β_{12}. Specifically, for every one unit ($MJm^{-2}d^{-1}$) increase in solar radiation, one might expect an increase of 0.05 g m^{-2}/g m^{-2} in the coefficient β_{nyb} that quantifies the association between wheat yield and NYB, with a 95% probability that this increase ranges between 0.006 and 0.098. Taking into account the range in solar radiation values for this dataset, the change in β_{nyb} can be expected to range from −0.13 to 0.09, on average, as a result of the effects of solar radiation. These values were obtained by multiplying the range for solar radiation values in the data with the median for β_{12}. Furthermore, posterior inference on β_{13} indicates a 96% probability for a positive contribution of precipitation to the expected rate of change of wheat yield as a function of NYB (i.e., β_{nyb}) during the early reproductive stage. The contribution of every unit of increased precipitation (cm) to β_{nyb} has a posterior median at 0.01 with a posterior standard deviation of 0.005. In context of this dataset, this effect on β_{nyb} can be expected to range from −0.12 to 0.09. In turn, evidence for a contribution of temperature (β_{11}) to the association between yield and NYB (i.e., β_{nyb}) was weaker, as the HDI for β_{11} shows substantial overlap with the null value zero and the posterior probability of a nonzero positive effect is approximately 70%.

Furthermore, the joint posterior densities for β_{12} and β_{13} indicate a strong correlation between the contributions of precipitation and that of solar radiation to β_{nyb}, that is, the rate of change of yield as a function of NYB during the early reproductive stage (Figure 3, right panel). Specifically, this correlation was estimated at 0.83, suggesting the possibility of multicollinearity between these weather contributors. In contrast, the estimated posterior correlations between the contributions of temperature (β_{11}) and any of the remaining weather variables (β_{12} and β_{13}) to β_{nyb} was small, at −0.06 and −0.01, respectively (Figure 3 left and center panels, respectively).

Table 5 also shows posterior inference on parameters β_{21}, β_{22}, β_{23}, which characterize the TKW-mediated contribution of temperature, solar radiation, and precipitation, respectively, to wheat yield during the grain filling stage thus providing further insight into source-sink balance. Specifically, posterior inference on β_{23} further indicates a 91% probability for a nonzero positive contribution of precipitation to the expected rate of change of wheat yield as a function of TKW (i.e., β_{tkw}) during the grain filling stage. The contribution of every unit of increased precipitation to β_{tkw} had a posterior median at 0.32 with a posterior standard deviation of 0.24. For this dataset, this effect on β_{tkw} can be expected to range from −2.36 to 4.73. By contrast, posterior inference for the remaining coefficients β_{21} and β_{22} showed 95% HDIs that overlapped with zero, thus suggesting little, if any, contributions of temperature and solar radiation to wheat yield through TKW, given the range of temperature in this dataset. In addition, posterior correlations between β_{21}, β_{22}, β_{23} during the grain filling stage were small in magnitude (below 0.25; Figure 4), suggesting negligible dependence between weather contributions to source mechanisms for wheat yield.

4 | DISCUSSION

In this study, we implemented a hierarchical Bayesian approach to model wheat yield in Oklahoma on an ecophysiological basis, that is, as a function of two yield

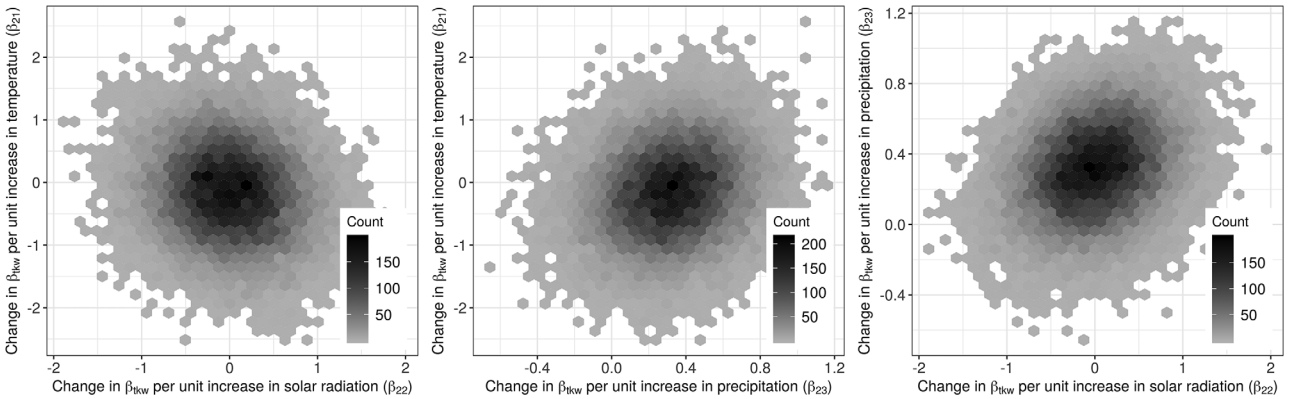

FIGURE 4 Pairwise joint posterior densities for parameters β_{21}, β_{22}, β_{23} characterizing the contribution of weather variables to the relationship between yield and thousand kernel weight during the grain filling stage

component traits related to source-sink relations, namely nonyield biomass (NYB) and thousand kernel weight (TKW). We further leveraged hierarchical models to assess the contribution of weather variables to the relationships between yield and yield component traits at different growth stages.

4.1 | Model comparison

Based on a combination of model fit criteria and hierarchical structure of the biological question of interest, we proceeded with inference using Model 3: GE-YC-hierarchy. In particular, Bayesian R-squared indicated that the selected model was well suited to fit the data, as its posterior density was centered at 0.89 with a lower HDI bound of 0.85. In addition, the estimated RMSE for this model was 67 g m^{-2}, which is within range of other reports in the literature ranging from as low as 10 g m^{-2} up to 150 g m^{-2} (Huang et al., 2016; Li et al., 2015; Kogan et al., 2013; Nain et al., 2004).

4.2 | Genotypic, environmental, and G × E interaction effects on yield

In this section, we interpret the changes in variance components for environment (σ^2_{env}), genotype (σ^2_{geno}) and G × E (σ^2_{ge}) interaction across alternative models, GE, GE-YC, and GE-YC-hierarchy. Recall that Model 1: GE did not account for yield component traits NYB and TKW. As a result, a large portion of the total variability likely fell to the environment. The posterior estimates for environmental variance decreased by an order of magnitude when yield component traits were added in Model 2: GE-YC and Model 3: GE-YC-hierarchy, indicating that a large proportion of the variance originally explained by the environment and left-over noise in Model 1: GE was explained by the yield component traits in Models 2: GE-YC and 3:GE-YC-hierarchy. The inclusion of yield components NYB and TKW in Models 2: GE-YC and 3:GE-YC-hierarchy were intended to help explain yield variation in terms of eco-physiological mechanisms. In turn, the similarity in magnitudes of variance estimates for genotypic and G × E components across all three models suggest that NYB and TKW do not explain the variance associated with genotype and G × E interaction effects.

For Model 3: GE-YC-hierarchy based on the point estimates (medians) of the posterior distributions for the variance components for genotypic, environmental, and G × E interaction effects (σ^2_{geno}, σ^2_{env}, and σ^2_{ge}, respectively), σ^2_{env} was found to be the largest by at least 6-fold (Table 4). In addition to this point estimate, the HDI for σ^2_{env} also indicates much larger lower and upper bounds compared with the HDIs for σ^2_{geno} and σ^2_{ge} (Table 4). This suggests that the environment (i.e., site-year) accounted for a considerable part of the total variability in wheat yield. This finding is in accordance with the literature whereby Munaro et al. (2020) showed that for Colorado, Kansas, and Oklahoma the environmental difference across years and locations accounted for 46% of yield variability. In context of the seasons and locations included in the study, different biotic and abiotic factors contributed to the differences in growing environments.

In terms of overall growing conditions, the growing season of 2016–2017 (i.e., harvest year 2017) reportedly showed optimal growing conditions (Marburger et al., 2017). However, during that season, the Chickasha site suffered a severe and early infection of leaf rust; this is probably the reason behind Chickasha 2016–2017 being the lowest yielding environment (Marburger et al., 2017). On the other hand, the growing conditions during the season of 2017–2018 in Oklahoma were characterized by overall cooler temperatures at early growth stages and record cold temperatures in April with a spring-freeze (Marburger, Calhoun, Carver, et al., 2018), thus resulting in slow growth and development of the crop (Marburger, Calhoun, Carver, et al., 2018). Weather conditions in Oklahoma were further compounded with hotter temperatures and lack of rainfall during the grain filling stage, including record hot temperatures

in May (Marburger, Calhoun, Carver, et al., 2018). In addition, the wheat variety trial plots in Lahoma were also affected by dryland root rot during the 2017–2018 season. Finally, the 2018–2019 growing season mostly had favorable growing conditions for both growth and development and grain filling stages, except for the occurrence of diseases such as root rot, black chaff, and powdery mildew in some locations (Calhoun et al., 2019). The locations under study are also different in their soil type and properties. However, the interannual variability within locations was observed to be higher than the spatial variability. These variations were characterized by biotic factors such as diseases and abiotic factors such as drought and spring freeze. The abiotic factors such as drought were captured by the model to some extent through inclusion of precipitation, but further work is required to analyze the other sources of variability between years and locations. Thus, further analysis should focus on exploring methods to incorporate the biotic stresses as well as the occasional abiotic stresses such as spring freeze.

The posterior medians for σ^2_{geno} and σ^2_{ge} were on a comparable order of magnitude indicating that genotypic effects, as well as G × E interaction effects, explain yield variability comparably. However, upon subsequent analysis, it was revealed that the probability of effect of genotype-specific effects on wheat yield is higher than the effect of G × E interaction. Although small, the G × E effects were manifested as reranking of genotypes across environments. For instance, SY Flint was ranked in the lowest half for yield in Altus_2018 (i.e., harvest year 2018) but ranked highly the following year, particularly in the Altus_2019 environment (Figure 2).

4.3 | Association between wheat yield and yield component traits

One of the objectives of this study was to model wheat yield as a function of yield component traits to be able to identify physiological mechanisms contributing to source-sink balance. Specifically, we used NYB as a source indicator because it is an independent measure of the source which does not contain the variable we are trying to predict (yield). Hence, it can be argued that NYB represents the source more clearly and uniquely than total crop biomass. Specifically, the ratio of yield to NYB can be expressed in terms of Harvest Index (HI) as $Yield/NYB = HI/(1 - HI)$. For clarity and detail, recall that $HI = Yield/Biomass$ and also, $NYB = Biomass - Yield$. One may then express $NYB/Yield = (Biomass - Yield)/Yield$, such that $NYB/yield = 1/(HI - 1)$, leading to re-expressing β_{nyb} as $Yield/NYB = HI/(1 - HI)$. This identity enabled us to draw connections between our study and the published literature. So defined, HI is commonly used to assess source-sink balance in wheat (Reynolds et al., 2017; Zhang et al., 2010).

The slope parameter connecting wheat yield and NYB, β_{nyb}, is equal to β_{10} at average weather conditions in Model 3: GE-YC-hierarchy. The HDI for β_{10} was (0.38, 0.47 g m^{-2}/g m^{-2}). The positive value of β_{nyb} indicates that source is one of the drivers for yield in these environments. Other studies have reported theoretical maximums for HI in wheat to be 0.62, 0.64, and 0.66 (Austin et al., 1980; Foulkes et al., 2011; Shearman et al., 2005). However, the HI for maximum attainable yields in the Southern Great Plains has been estimated at not more than 0.41 (Lollato & Edwards, 2015). In addition, a survey on five different classes of wheat across the United States reported the HI of hard red winter wheat (the most commonly grown wheat in Oklahoma) to be 0.33, the lowest among all wheat classes (Dai et al., 2016). An HI far lower than the attainable HI suggests that yield increase could be achieved through better utilization of available source through improved dry matter partitioning.

Further, our results indicate a positive slope coefficient between wheat yield and TKW (i.e., β_{tkw} in Model GE-YC-hierarchy), suggesting that the genotypes in this population did not consistently achieve their genetic potential for TKW across environments. This finding could be interpreted as an insufficient source to match the sink strength, thus a source–sink imbalance in the population within many of the target environments. The TKW is generally a stable trait with high heritability. Moreover, we had expected that some portion of the genotypic variance would be explained by the yield component TKW, as this trait is generally considered to vary more between genotypes than between environments (Sadras, 2007). This expectation is based on the understanding that wheat is generally considered to be a sink-limited crop under many conditions (Alonso et al., 2018; Serrago et al., 2013; Zhang et al., 2010; Slafer & Savin, 1994). When the yield is sink-limited, genetic potential TKW is consistently achieved, the yield is limited by grain number, and the relationship between yield and TKW is at or near zero (Reynolds et al., 2005; Slafer et al., 2014). However, when source limitation is at play, differences in TKW across environments would be greater than differences between genotypes, resulting in a nonzero slope for the relationship between yield and TKW. Thus, our findings of a positive slope for TKW and a positive slope between yield and NYB (i.e., an increase in yield with an increase in the source) both point toward source limitation for yield.

4.4 | Contribution of weather variables in the relationships between yield and yield component traits

We incorporated the weather variables as hierarchical regressors that qualify the nature of the relationship between yield

and each of NYB and TKW, thus extending Model 2: GE-YC to Model 3: GE-YC-hierarchy. If the inclusion of hierarchical levels to account for weather variables made any contribution to explaining noise in the data, this contribution seemed to be mild at best, as the posterior density for the residual variance was only slightly decreased in magnitude from Model 2: GE-YC to Model 3: GE-YC-hierarchy (Table 4). This is not necessarily surprising as the explanatory role of weather was not at the first hierarchical level of the model; rather, weather variables were fitted at a second level of the model hierarchy, thus intended for a decomposition of the slopes connecting wheat yield to TKW and NYB. The hierarchical structure of the model allowed us to evaluate the contributions of weather conditions to the rate of change of wheat yield as a function of yield component traits. For the early reproductive stage, the effects of solar radiation (β_{12}) and precipitation (β_{13}) on the slope of yield vs. NYB (β_{nyb}) were positive. It is noted that these two effects were also tightly correlated with each other a posteriori. This is consistent with the previously reported relationship between radiation use efficiency and water use efficiency (Caviglia & Sadras, 2001; Sadras et al., 1991). Specifically, a positive correlation of substantial magnitude was reported between cumulative water consumed and photosynthetically active radiation intercepted in durum wheat (Rezig et al., 2015).

Conditions of both higher solar radiation and adequate rainfall are considered favorable for plant growth. Higher solar radiation corresponds to increased photosynthesis and higher assimilate supply, and higher rainfall ensures no drought stress. Therefore, the observed positive effects of solar r diation and precipitation during the early reproductive stage (β_{12} and β_{13}) on the rate of change of yield per NYB (β_{nyb}) indicate that the amount of yield produced per unit NYB is higher under favorable conditions. These findings can be interpreted as the source (NYB) being used more efficiently for yield formation as a result of better sink strength, given that this is a period when florets are developing and, thus, grain number is determined (Ugarte et al., 2007; Savin & Slafer, 1991; Fischer, 1985).

For the grain filling stage, only precipitation was found to contribute to the rate of yield change per TKW (β_{20}), although the evidence was weaker (i.e., posterior probability $P[\beta_{23} > 0|y] = 70\%$). The positive slope between yield and TKW indicating potential source limitation during grain filling and the weak evidence of weather variables contributing to that points toward other factors that might affect source strength during grain filling, such as disease or residual soil moisture. In turn, the evidence of the precipitation effect, although weak, is consistent with a report that the effect of precipitation during the grain filling stage on wheat yield was mainly mediated by TKW (He et al., 2013).

5 | CONCLUSION

A major portion of the total variability in wheat yield was explained by the environmental component. The inclusion of yield component traits, namely NYB and TKW, as explanatory variables in the model helped explained a substantial amount of environmental variance but did not seem to help explain genotypic or G × E variance. A positive relationship was observed between both yield component traits and wheat yield supporting the idea that yield is driven by source mechanisms. However, the fact that the slope of yield as a function of NYB was responsive to weather conditions during the early reproductive stage indicates that sink mechanisms may also be at play. These results suggest the presence of source-sink co-limitation in wheat yield.

ACKNOWLEDGMENTS

We thank Andrew Baird, Dr. Uvirkaa Akumaga, Blake Macnelly, Brandon Vaverka, Robert Calhoun, Nathan Stepp, and Tina Johnson for their assistance in data collection, and Evan Linde for technical support. We also thank the Oklahoma Wheat Commission and the Oklahoma Wheat Research Foundation for providing partial funding for this research. This research was supported in part by National Science Foundation under Grant No. OIA-1301789 and OIA-1826820.

AUTHOR CONTRIBUTIONS

Pratishtha Poudel: Conceptualization; Data curation; Formal analysis; Investigation; Methodology; Writing-original draft; Writing-review & editing. Nora M. Bello: Formal analysis; Methodology; Supervision; Writing-review & editing. David A. Marburger: Conceptualization; Resources; Writing-review & editing. Brett F. Carver: Resources; Writing-review & editing. Ye Liang: Methodology; Writing-review & editing. Phillip Alderman: Conceptualization; Formal analysis; Funding acquisition; Project administration; Supervision; Writing-review & editing.

CONFLICT OF INTEREST

The authors declare no conflict of interest.

ORCID

David A. Marburger https://orcid.org/0000-0003-1342-4147

Brett F. Carver https://orcid.org/0000-0001-6800-5754

Phillip D. Alderman https://orcid.org/0000-0003-1467-2337

REFERENCES

Alderman, P. D., & Stanfill, B. (2017). Quantifying model-structure- and parameter-driven uncertainties in spring wheat phenology prediction with Bayesian analysis. *European Journal of Agronomy*, *88*, 1–9. https://doi.org/10.1016/j.eja.2016.09.016

Alonso, M. P., Abbate, P. E., Mirabella, N. E., Merlos, F. A., Panelo, J. S., & Pontaroli, A. C. (2018). Analysis of sink/source relations in bread wheat recombinant inbred lines and commercial cultivars under a high yield potential environment. *European Journal of Agronomy*, *93*, 82–87. https://doi.org/10.1016/j.eja.2017.11.007

Austin, R. B., Bingham, J., Blackwell, R. D., Evans, L. T., Ford, M. A., Morgan, C. L., & Taylor, M. (1980). Genetic improvements in winter wheat yields since 1900 and associated physiological changes. *The Journal of Agricultural Science*, *94*(3), 675–689. https://doi.org/10.1017/S0021859600028665

Borrás, L., Slafer, G. A., & Otegui, M. E. (2004). Seed dry weight response to source–sink manipulations in wheat, maize and soybean: A quantitative reappraisal. *Field Crops Research*, *86*(2–3), 131–146. https://doi.org/10.1016/j.fcr.2003.08.002

Brock, F. V., Crawford, K. C., Elliott, R. L., Cuperus, G. W., Stadler, S. J., Johnson, H. L., & Eilts, M. D. (1995). The Oklahoma Mesonet: A technical overview. *Journal of Atmospheric and Oceanic Technology*, *12*(1), 5–19. https://doi.org/10.1175/1520-0426(1995)012%3c0005:TOMATO%3e2.0.CO;2

Calhoun, R., Carver, B., Hunger, B., Edwards, J., Watson, B., & Gillespie, C. (2019). *2017–18 small grains variety performance tests, CR-2143 Rev. 0819*. Oklahoma State University.

Caviglia, O. P., & Sadras, V. O. (2001). Effect of nitrogen supply on crop conductance, water-and radiation-use efficiency of wheat. *Field Crops Research*, *69*(3), 259–266. https://doi.org/10.1016/S0378-4290(00)00149-0

Cotes, J. M., Crossa, J., Sanches, A., & Cornelius, P. L. (2006). A Bayesian approach for assessing the stability of genotypes. *Crop Science*, *46*(6), 2654–2665. https://doi.org/10.2135/cropsci2006.04.0227

Cuevas, J., Crossa, J., Montesinos-López, O. A., Burgueño, J., Pérez-Rodríguez, P., & de los Campos, G. (2017). Bayesian genomic prediction with genotype × environment interaction kernel models. *G3: Genes, Genomes, Genetics*, *7*(1), 41–53. https://doi.org/10.1534/g3.116.035584

Dai, J., Bean, B., Brown, B., Bruening, W., Edwards, J., Flowers, M., Karow, R., Lee, C., Morgan, G., Ottman, M., Ransom, J., & Wiersma, J. (2016). Harvest index and straw yield of five classes of wheat. *Biomass and Bioenergy*, *85*, 223–227. https://doi.org/10.1016/j.biombioe.2015.12.023

Edwards, J. T., Hunger, R. M., Smith, E. L., Horn, G. W., Chen, M. S., Yan, L., Bai, G., Bowden, R. L., Klatt, A. R., Rayas-Duarte, P., Osburn, R. D., Giles, K. L., Kolmer, J. A., Jin, Y., Porter, D. R., Seabourn, B. W., Bayles, M. B., & Carver, B. F. (2012). 'Duster' wheat: A durable, dual-purpose cultivar adapted to the southern Great Plains of the USA. *Journal of Plant Registrations*, *6*(1), 37–48. https://doi.org/10.3198/jpr2011.04.0195crc

Fischer, R. A. (1985). Number of kernels in wheat crops and the influence of solar radiation and temperature. *Journal of Agricultural Science*, *105*(2), 447–461. https://doi.org/10.1017/S0021859600056495

Fischer, R. A. (2008). The importance of grain or kernel number in wheat: A reply to Sinclair and Jamieson. *Field Crops Research*, *105*(1–2), 15–21. https://doi.org/10.1016/j.fcr.2007.04.002

Foulkes, M. J., Slafer, G. A., Davies, W. J., Berry, P. M., Sylvester-Bradley, R., Martre, P., Calderini, D. F., Griffiths, S., & Reynolds, M. P. (2011). Raising yield potential of wheat. iii. optimizing partitioning to grain while maintaining lodging resistance. *Journal of Experimental Botany*, *62*(2), 469–486. https://doi.org/10.1093/jxb/erq300

Gelman, A., Carlin, J. B., Stern, H. S., Dunson, D. B., Vehtari, A., & Rubin, D. B. (2013). *Bayesian data analysis*. CRC Press.

Gelman, A., Goodrich, B., Gabry, J., & Vehtari, A. (2019). R-squared for Bayesian regression models. *The American Statistician*, *73*(3), 307–309. https://doi.org/10.1080/00031305.2018.1549100

Grieve, A. P. (1991). On the construction of shortest confidence intervals and Bayesian highest posterior density intervals. *Journal of Veterinary Pharmacology and Therapeutics*, *14*(4), 395–399. https://doi.org/10.1111/j.1365-2885.1991.tb00853.x

He, Y., Wei, Y., DePauw, R., Qian, B., Lemke, R., Singh, A., Cuthbert, R., McConkey, B., & Wang, H. (2013). Spring wheat yield in the semiarid Canadian prairies: Effects of precipitation timing and soil texture over recent 30 years. *Field Crops Research*, *149*, 329–337. https://doi.org/10.1016/j.fcr.2013.05.013

Huang, J., Sedano, F., Huang, Y., Ma, H., Li, X., Liang, S., Tian, L., Zhang, X., Fan, J., & Wu, W. (2016). Assimilating a synthetic Kalman filter leaf area index series into the WOFOST model to improve regional winter wheat yield estimation. *Agricultural and Forest Meteorology*, *216*, 188–202. https://doi.org/10.1016/j.agrformet.2015.10.013

Hunger, R. M., Edwards, J. T., Bowden, R. L., Yan, L., Rayas-Duarte, P., Bai, G., Horn, G. W., Kolmer, J. A., Giles, K. L., Chen, M. - S., Jin, Y., Osburn, R. D., Bayles, M. B., Seabourn, B. W., Klatt, A. R., & Carver, B. F. (2014). 'Billings' wheat combines early maturity, disease resistance, and desirable grain quality for the southern Great Plains, USA. *Journal of Plant Registrations*, *8*(1), 22–31. https://doi.org/10.3198/jpr2012.11.0053crc

Kaya, Y., Akcura, M., Ayranci, R., & Taner, S. (2006). Pattern analysis of multi-environment trials in bread wheat. *Communications in Biometry Crop Science*, *1*(1), 63–71.

Kogan, F., Kussul, N., Adamenko, T., Skakun, S., Kravchenko, O., Kryvobok, O., Shelestov, A., Kolotii, A., Kussul, O., & Lavrenyuk, A. (2013). Winter wheat yield forecasting in Ukraine based on Earth observation, meteorological data and biophysical models. *International Journal of Applied Earth Observation and Geoinformation*, *23*, 192–203. https://doi.org/10.1016/j.jag.2013.01.002

Li, Z., Jin, X., Zhao, C., Wang, J., Xu, X., Yang, G., Li, C., & Shen, J. (2015). Estimating wheat yield and quality by coupling the DSSAT-CERES model and proximal remote sensing. *European Journal of Agronomy*, *71*, 53–62. https://doi.org/10.1016/j.eja.2015.08.006

Lollato, R. P., & Edwards, J. T. (2015). Maximum attainable wheat yield and resource-use efficiency in the southern Great Plains. *Crop Science*, *55*(6), 2863–2876. https://doi.org/10.2135/cropsci2015.04.0215

Marburger, D., Calhoun, R., Beedy, T., Carver, B., Hunger, B., Watson, B., & Gillespie, C. (2017). *2016–17 Small grains variety performance tests, CR-2143 Rev. 0917*. Oklahoma State University. http://wheat.okstate.edu/variety-testing/grain-yield-previous-yrs/CR2143web2017.pdf

Marburger, D., Calhoun, R., Carver, B., Hunger, B., Watson, B., & Gillespie, C. (2018). *2017–18 Small grains variety performance tests, CR-2143 Rev. 0718*. Oklahoma State University. http://wheat.okstate.edu/variety-testing/grain-yield-previous-yrs/cr-2143web2018-small-grains-vt

Marburger, D., Hunger, B., Carver, B., & Royer, T. (2018). *Wheat variety comparison, PSS-2142*. Oklahoma State University. http://pods.dasnr.okstate.edu/docushare/dsweb/Get/Document-6107/PSS-2142web2018.pdf

Marburger, D. A., Silva, A. D. O., Hunger, R. M., Edwards, J. T., van der Laan, L., Blakey, A. M., Kan, C.-C., Garland-Campbell, K.A., Bowden, R. L., Yan, L., Tilley, M., Chen, M.-S., Chen, Y. R., Bai, G., Jin, Y., Kolmer, J. A., Seabourn, B. W., Davila-El Rassi, G., Rayas-Duarte, P., Kerr, R. M., Carver, B. F. (2021). 'Gallagher'and 'Iba' hard red winter wheat: Half-sibs inseparable by yield gain, separable by producer preference. *Journal of Plant Registrations*, *15*(1), 177–195. https://doi.org/10.1002/plr2.20116

Martin, C. R., Rousser, R., & Brabec, D. L. (1993). Development of a single-kernel wheat characterization system. *Transactions of the ASAE*, *36*(5), 1399–1404. https://doi.org/10.13031/2013.28477

McPherson, R. A., Fiebrich, C. A., Crawford, K. C., Kilby, J. R., Grimsley, D. L., Martinez, J. E., Basara, J. B., Illston, B. G., Morris, D. A., Kloesel, K. A., Melvin, A. D., Shrivastava, H., Wolfinbarger, J. M., Bostic, J. P., Demko, D. B., Elliott, R. L., Stadler, S. J., Carlson, J. D., & Sutherland, A. J. (2007). Statewide monitoring of the mesoscale environment: A technical update on the Oklahoma Mesonet. *Journal of Atmospheric and Oceanic Technology*, *24*(3), 301–321. https://doi.org/10.1175/JTECH1976.1

Meredith, M., & Kruschke, J. (2018). *HDInterval: Highest (posterior) density intervals*. R package version 0.2.0. https://CRAN.R-project.org/package=HDInterval

Mohammadi, R., Roustaii, M., Haghparast, R., Roohi, E., Solimani, K., Ahmadi, M. M., Abedi, G. R., & Amri, A. (2010). Genotype × environment interactions for grain yield in rainfed winter wheat multi-environment trials in iran. *Agronomy Journal*, *102*(5), 1500–1510. https://doi.org/10.2134/agronj2010.0062

Montesinos-López, O. A., Montesinos-López, A., Hernández, M. V., Ortiz-Monasterio, I., Pérez-Rodríguez, P., Burgueño, J., & Crossa, J. (2019). Multivariate Bayesian analysis of on-farm trials with multiple-trait and multiple-environment data. *Agronomy Journal*, *111*(6), 2658–2669. https://doi.org/10.2134/agronj2018.06.0362

Munaro, L. B., Hefley, T. J., DeWolf, E., Haley, S., Fritz, A. K., Zhang, G., Haag, L. A., Schlegel, A. J., Edwards, J. T., Marburger, D., Alderman, P., Jones-Diamond, S. M., Johnson, J., Lingenfelser, J. E., Uneda-Trevisoli, S. H., & Lollato, R. P. (2020). Exploring long-term variety performance trials to improve environment-specific genotype × management recommendations: A case-study for winter wheat. *Field Crops Research*, *255*, 107848. https://doi.org/10.1016/j.fcr.2020.107848

Nain, A. S., Dadhwal, V. K., & Singh, T. P. (2004). Use of CERES-wheat model for wheat yield forecast in central Indo-Gangetic Plains of India. *The Journal of Agricultural Science*, *142*(1), 59. https://doi.org/10.1017/S0021859604004022

Osborne, B. G., & Anderssen, R. S. (2003). Single-kernel characterization principles and applications. *Cereal Chemistry*, *80*(5), 613–622. https://doi.org/10.1094/CCHEM.2003.80.5.613

OSU Small Grains Extension (2020). *Variety Characteristics*. Oklahoma State University. http://wheat.okstate.edu/variety-characteristics-1/variety-characteristics

Peña-Bautista, R. J., Hernandez-Espinosa, N., Jones, J. M., Guzmán, C., & Braun, H. J. (2017). CIMMYT series on carbohydrates, wheat, grains, and health: Wheat-based foods: Their global and regional importance in the food supply, nutrition, and health. *Cereal Foods World*, *62*(5), 231–249. https://doi.org/10.1094/CFW-62-5-0231

Perten Instruments. (1995). SKCS 4100 Single Kernel Characterization System. *Instruction Manual*.

R Core Team (2020). *R: A language and environment for statistical computing*. R Foundation for Statistical Computing. https://www.R-project.org/

Ray, D. K., Gerber, J. S., MacDonald, G. K., & West, P. C. (2015). Climate variation explains a third of global crop yield variability. *Nature Communications*, *6*(1), 1–9. https://doi.org/10.1038/ncomms6989

Reynolds, M. P., Pask, A. J. D., Hoppitt, W. J. E., Sonder, K., Sukumaran, S., Molero, G., Pierre, C. S., Payne, T., Singh, R. P., Braun, H. J., Gonzalez, F. G., Terrile, I. I., Barma, N. C. D., Hakim, A., He, Z., Fan, Z., Novoselovic, D., Maghraby, M., Gad, K. I. M., …, & Joshi, A. K. (2017). Strategic crossing of biomass and harvest index—source and sink—achieves genetic gains in wheat. *Euphytica*, *213*(11), 257. https://doi.org/10.1007/s10681-017-2040-z

Reynolds, M. P., Pellegrineschi, A., & Skovmand, B. (2005). Sink-limitation to yield and biomass: A summary of some investigations in spring wheat. *Annals of Applied Biology*, *146*(1), 39–49. https://doi.org/10.1111/j.1744-7348.2005.03100.x

Rezig, M., M'hamed, H. C., & Naceur, M. B. (2015). Durum wheat (*Triticum durum* desf): Relation between photosynthetically active radiation intercepted and water consumption under different nitrogen rates. *Journal of Agricultural Science*, *7*(8), 225. https://doi.org/10.5539/jas.v7n8p225

Roozeboom, K. L., Schapaugh, W. T., Tuinstra, M. R., Vanderlip, R. L., & Milliken, G. A. (2008). Testing wheat in variable environments: Genotype, environment, interaction effects, and grouping test locations. *Crop Science*, *48*(1), 317–330. https://doi.org/10.2135/cropsci2007.04.0209

Sadras, V. O. (2007). Evolutionary aspects of the trade-off between seed size and number in crops. *Field Crops Research*, *100*(2-3), 125–138. https://doi.org/10.1016/j.fcr.2006.07.004

Sadras, V. O., & Slafer, G. A. (2012). Environmental modulation of yield components in cereals: Heritabilities reveal a hierarchy of phenotypic plasticities. *Field Crops Research*, *127*, 215–224. https://doi.org/10.1016/j.fcr.2011.11.014

Sadras, V. O., Whitfield, D. M., & Connor, D. J. (1991). Transpiration efficiency in crops of semi-dwarf and standard-height sunflower. *Irrigation Science*, *12*(2), 87–91. https://doi.org/10.1007/BF00190015

Savin, R., & Slafer, G. A. (1991). Shading effects on the yield of an argentinian wheat cultivar. *Journal of Agricultural Science*, *116*(1), 1–7. https://doi.org/10.1017/S0021859600076085

Schad, D. J., Betancourt, M., & Vasishth, S. (2019). Toward a principled Bayesian workflow in cognitive science. *arXiv*.

Serrago, R. A., Alzueta, I., Savin, R., & Slafer, G. A. (2013). Understanding grain yield responses to source–sink ratios during grain filling in wheat and barley under contrasting environments. *Field Crops Research*, *150*, 42–51. https://doi.org/10.1016/j.fcr.2013.05.016

Serrago, R. A., & Miralles, D. J. (2014). Source limitations due to leaf rust (caused by *Puccinia triticina*) during grain filling in wheat. *Crop and Pasture Science*, *65*(2), 185–193. https://doi.org/10.1071/CP13248

Shearman, V. J., Sylvester-Bradley, R., Scott, R. K., & Foulkes, M. J. (2005). Physiological processes associated with wheat yield progress in the UK. *Crop Science*, *45*(1), 175–185.

Slafer, G. A., & Savin, R. (1994). Postanthesis green area duration in a semidwarf and a standard-height wheat cultivar as affected by sink strength. *Australian Journal of Agricultural Research*, *45*(7), 1337–1346. https://doi.org/10.1071/AR9941337

Slafer, G. A., Savin, R., & Sadras, V. O. (2014). Coarse and fine regulation of wheat yield components in response to genotype and

environment. *Field Crops Research*, *157*, 71–83. https://doi.org/10.1016/j.fcr.2013.12.004

Stan Development Team. (2018). *Stan modeling language users guide and reference manual* (version 2.18.0). http://mc-stan.org

Stan Development Team. (2019). *RStan: The R interface to Stan* (R package version 2.19.2). http://mc-stan.org/

Sukumaran, S., Crossa, J., Jarquin, D., & Reynolds, M. (2017). Pedigree-based prediction models with genotype × environment interaction in multienvironment trials of CIMMYT wheat. *Crop Science*, *57*(4), 1865–1880. https://doi.org/10.2135/cropsci2016.06.0558

Tian, L., & Quiring, S. M. (2019). Spatial and temporal patterns of drought in Oklahoma (1901–2014). *International Journal of Climatology*, *39*(7), 3365–3378. https://doi.org/10.1002/joc.6026

Ugarte, C., Calderini, D. F., & Slafer, G. A. (2007). Grain weight and grain number responsiveness to pre-anthesis temperature in wheat, barley and triticale. *Field Crops Research*, *100*(2-3), 240–248. https://doi.org/10.1016/j.fcr.2006.07.010

USDA. (2019). *Oklahoma agricultural statistics*. https://www.nass.usda.gov/Statistics_by_State/Oklahoma/Publications/Annual_Statistical_Bulletin/ok-bulletin-2019.pdf

Vehtari, A., Gelman, A., & Gabry, J. (2017). Practical Bayesian model evaluation using leave-one-out cross-validation and WAIC. *Statistics and Computing*, *27*(5), 1413–1432. https://doi.org/10.1007/s11222-016-9696-4

Wardlaw, I. F., & Moncur, L. (1995). The response of wheat to high temperature following anthesis. i. the rate and duration of kernel filling. *Functional Plant Biology*, *22*(3), 391–397. https://doi.org/10.1071/PP9950391

Wickham, H. (2016). ggplot2*:* Elegant Graphics for Data Analysis. Springer-Verlag. https://ggplot2.tidyverse.org

Wickham, H. (2017). *tidyverse: Easily install and load the 'tidyverse'* (R package version 1.2.1). https://CRAN.R-project.org/package=tidyverse

Wickham, H., Averick, M., Bryan, J., Chang, W., McGowan, L. D., François, R., Grolemund, G., Hayes, A., Henry, L., Hester, J., Kuhn, M., Pedersen, T. L., Miller, E., Bache, S. M., Müller, K., Ooms, J., Robinson, D., Seidel, D. P., Spinu, V., … Yutani, H. (2019). Welcome to the tidyverse. *Journal of Open Source Software*, *4*(43), 1686. https://doi.org/10.21105/joss.01686

Xie, Y. (2020). *knitr: A general-purpose package for dynamic report generation in R* (R package version 1.29). https://yihui.org/knitr/

Zhang, H., Turner, N. C., & Poole, M. L. (2010). Source–sink balance and manipulating sink–source relations of wheat indicate that the yield potential of wheat is sink-limited in high-rainfall zones. *Crop and Pasture Science*, *61*(10), 852–861. https://doi.org/10.1071/CP10161

Zhu, H. (2019). *kableExtra: Construct complex table with 'kable' and pipe syntax* (R package version 1.1.0). https://CRAN.R-project.org/package=kableExtra

How to cite this article: Poudel, P., Bello, N. M., Marburger, D. A., Carver, B. F., Liang, Y., & Alderman, P. D. (2022) Ecophysiological modeling of yield and yield components in winter wheat using hierarchical Bayesian analysis. *Crop Science*, *62,* 358–373. https://doi.org/10.1002/csc2.20652